Decoding human motor activity from EEG single trials for a discrete two-dimensional cursor control



2009 J. Neural Eng. 6 046005

(http://iopscience.iop.org/1741-2552/6/4/046005)

J. Neural Eng. **6** (2009) 046005 (12pp) doi:10.1088/1741-2560/6/4/046005

# Decoding human motor activity from EEG single trials for a discrete two-dimensional cursor control

**Dandan Huang[1], Peter Lin[2], Ding-Yu Fei[1], Xuedong Chen[3] and Ou Bai[1,4]**

[1] Department of Biomedical Engineering, Virginia Commonwealth University, Richmond, VA 23284, USA
[2] Human Motor Control Section, Medical Neurological Branch, National Institute of Neurological Disorders, National Institutes of Health, Bethesda, MD 20892, USA
[3] School of Mechanical Science and Engineering, Huazhong University of Science and Technology, Wuhan, Hubei, 430074, People's Republic of China

E-mail: obai@vcu.edu

Received 16 March 2009
Accepted for publication 1 June 2009
Published 25 June 2009
Online at stacks.iop.org/JNE/6/046005

**Abstract**
This study aims to explore whether human intentions to move or cease to move right and left hands can be decoded from spatiotemporal features in non-invasive EEG in order to control a discrete two-dimensional cursor movement for a potential multidimensional brain–computer interface (BCI). Five naïve subjects performed either sustaining or stopping a motor task with time locking to a predefined time window by using motor execution with physical movement or motor imagery. Spatial filtering, temporal filtering, feature selection and classification methods were explored. The performance of the proposed BCI was evaluated by both offline classification and online two-dimensional cursor control. Event-related desynchronization (ERD) and post-movement event-related synchronization (ERS) were observed on the contralateral hemisphere to the hand moved for both motor execution and motor imagery. Feature analysis showed that EEG beta band activity in the contralateral hemisphere over the motor cortex provided the best detection of either sustained or ceased movement of the right or left hand. The offline classification of four motor tasks (sustain or cease to move right or left hand) provided 10-fold cross-validation accuracy as high as 88% for motor execution and 73% for motor imagery. The subjects participating in experiments with physical movement were able to complete the online game with motor execution at an average accuracy of 85.5 ± 4.65%; the subjects participating in motor imagery study also completed the game successfully. The proposed BCI provides a new practical multidimensional method by noninvasive EEG signal associated with human natural behavior, which does not need long-term training.

(Some figures in this article are in colour only in the electronic version)

## 1. Introduction

The brain–computer interface (BCI) provides a new means of direct brain communication with the external environment for patients who may partly or entirely lose voluntary muscle contraction such as in the 'locked-in' state (Birbaumer *et al* 2008). One of the most useful applications for BCI is to control an external device, e.g., wheelchair or robotic arms, to restore motor function (Leeb *et al* 2007). This purpose requires a BCI capable of multidimensional control. Although multidimensional control is highly promising using invasive methods, e.g. local field potentials/spike train (Lebedev and Nicolelis 2006, Velliste *et al* 2008), or semi-invasive methods using electrocorticography (ECoG) (Schalk *et al* 2008), the noninvasive methods, in particular,

[4] Author to whom any correspondence should be addressed.

 

electroencephalography (EEG), mainly support the one-dimensional control (Krusienski *et al* 2007, McFarland and Wolpaw 2003). Successful two-dimensional BCI using noninvasive EEG signals has been achieved (Wolpaw and McFarland 2004). However, the subjects needed long-term training, up to several months, before they could reliably attain two-dimensional BCI control.

Recent studies have developed a scheme to achieve two-dimensional control by sequentially combining two binary controls (Bai *et al* 2007, 2008). Though sequential combination of one-dimensional control may achieve two-dimensional control, direct two-dimensional control, i.e., a simultaneous control of four directions in a two-dimensional plane, will be more effective, and thus, more convenient for use.

Human somatotopic organization indicates that human limbs are controlled by contralateral brain hemispheres. Many neurophysiological and neuroimaging studies have confirmed the nature of contralateral control (Bai *et al* 2005, Rao *et al* 1993, Stancak and Pfurtscheller 1996). Therefore, reliably decoding the movement intention of right and left hands, which are associated with different spatiotemporal patterns of event-related desynchronization (ERD), i.e. oscillation amplitude attenuation, and event-related synchronization (ERS), i.e. oscillation amplitude increase, may provide additional degrees-of-freedom for control. During physical and motor imagery of right- and left-hand movements, beta band brain activation (15–30 Hz) ERD occurs predominantly over the contralateral left and right motor areas. The brain activity associated with ceasing to move, the post-movement ERS, can also be found over the contralateral motor areas. It suggests that the brain activity associated with four natural motor behaviors (thus, not requiring training) may potentially provide four reliable features for a discrete two-dimensional control, e.g. left-hand ERD to command to move left, left-hand ERS to command move up, right-hand ERD to command to move right and right-hand ERS to command move down. As the spatial distribution of post-movement beta rebound (ERS) is more focal than ERD distribution, the detection of ERS might potentially be more reliable than the ERD detection only (Pfurtscheller and Solis-Escalante 2009). As a result, the proposed method to discriminate the spatial distribution of ERD and ERS might provide more accurate classification than previous methods relying on the detection of ERD only (Neuper *et al* 2005, Naeem *et al* 2006). Although evidence has demonstrated separate spatial patterns of ERD and ERS with physical movement, it is also important to know about the hemispheric patterns during motor imagery of limb movement which is essential for achieving purely mental control without involvement of muscle activity.

In summary, the aim of this study is to introduce a novel BCI paradigm/method: decoding ERD and ERS associated with natural motor behavior so that the subjects can control cursor movement in a two-dimensional plane with minimal training. We have tested whether the decoding of multiple movement intentions is reliable enough to control a two-dimensional computer cursor for a possible multidimensional brain–computer interface (BCI). We also employed advanced signal processing and classification methods for better decoding of human intentions from single trial EEG to improve the performance of the proposed BCI paradigm. The reliability of two-dimensional cursor control has been tested on a virtual online computer game.

## 2. Method

### 2.1. Subjects

Five healthy volunteers (three females and two males) between the ages of 20 and 27 participated in this study. They were right handed according to the Edinburgh inventory (Oldfield 1971). All subjects gave informed consent. Prior to this study, none of these subjects had been exposed to a BCI system or were informed of the experimental hypothesis. The protocol was approved by the Institutional Review Board.

### 2.2. Experimental paradigm

The experimental paradigm in this study was similar to a previous study (Bai *et al* 2008). All subjects participated in the first session of the study, i.e. motor execution with physical movement. Two subjects (S1 and S2) were also available to further participate in the second session, i.e. motor imagery.

During recording, a quiet environment with dim light was provided to maintain the subjects' attention level. The subjects were seated in a chair with the forearms semi-flexed and supported by a pillow. They were asked to keep all muscles relaxed, except for those in the performing arms; besides, they were also instructed to avoid eye movements, blinks, body adjustments, swallowing or other movements during the visual cue onset. During motor imagery, the investigator monitored the EMG activity continuously; once EMG activity was observed, the subjects were reminded to relax the muscles. Trials with EMG contamination were excluded based on visual inspection for further offline ERD and ERS feature analysis and classification. Visual inspection was done by inspecting continuous EEG data. For EEG recordings associated with physical movement, trials with EMG activities presented in both right and left hands, i.e., bilateral movements, were excluded. For EEG data with motor imagery, trials with EMG activities spreading in EEG channels due to facial muscle contraction were excluded. Each of the motor execution with physical movement and motor imagery sessions contained an initial calibration step to determine the optimal frequency band and spatial channels. The selected features and generated model were then used to test an online two-dimensional-cursor-control game. The two sessions were performed continuously within 3–4 h in a single visit.

*2.2.1. Calibration.* Visual stimuli were periodically presented on a computer screen, placed in front of the subjects, with the distance and the height adjusted for the subject's comfort. In the first session (pure physical movement), there were four cues in the task paradigm, 'RYes', 'RNo', 'LYes' and 'LNo' ('R' indicates the right-hand task, and 'L' for the left-hand task). The visual cue was displayed for a period

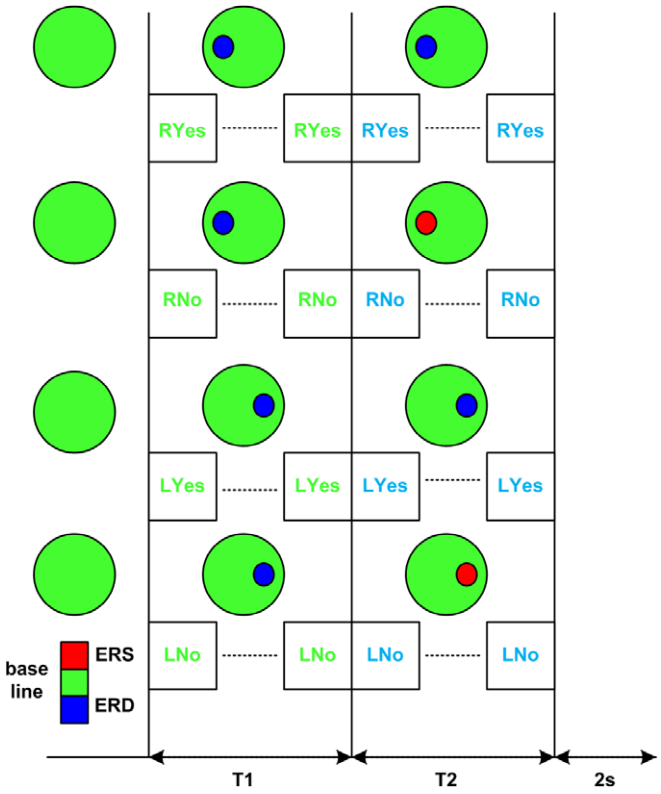


**Figure 1.** Calibration paradigm. In the case of 'RYes', the subjects were instructed to start motor execution or motor imagery using right hand when the first cue presented (green color) at the beginning of the T1 window; when the color of cue turned to blue at the beginning of the T2 window, the subjects were instructed to sustain motor execution or motor imagery (ERD by a small blue circle was expected on the left hemisphere, see detail in the text). In the case of 'RNo', the subjects were instructed to start motor execution or motor imagery using right hand when the first cue presented (green color) at the beginning of the T1 window; when the color of cue turned to blue at the beginning of the T2 window, the subjects were instructed to stop motor execution or motor imagery (ERS by small red circle was expected on the left hemisphere). Procedures were similar for 'LYes' and 'LNo' with left-hand motor execution or motor imagery.

of T1 in green color, followed by a color change of the cue to blue, which is illustrated in figure 1. The second cue was displayed for a period of T2, after which the cue disappeared. The lengths of the T1 and T2 windows were set to 2.5 s initially. The time interval between the end of T2 and the next T1, i.e. trial-to-trial interval, was set to 2 s. The subjects were instructed to begin repetitive wrist extensions of the right arm at the onset of the initial cue 'RYes' or 'RNo'. At the time of color change, the subject was instructed to continue movement with the 'Yes' cue or abruptly relax and stop moving with the 'No' cue. The task was similar for 'LYes' and 'LNo', where the subjects performed using the left hand instead.

In the calibration step for motor imagery, the subjects were asked to perform both physical movement and motor imagery according to eight cues: 'PHYRYes', 'PHYRNo', 'PHYLYes', 'PHYLNo' (for physical movement) and 'MIRYes', 'MIRNo', 'MILYes', 'MILNo' (for motor imagery). The alternation of physical movement and motor imagery was intended to provide the subject with a vivid mental sensation of physical movement for better motor imagery. The visual cues were randomly presented, and the subject performed either physical movement or motor imagery, using either right or left hand, following the instruction of the ongoing cue. The lengths of T1 and T2 were adjusted according to the different response delays for each subject, and kept consistent in the following sessions/steps.

The calibration procedure for the physical movement session consisted of three or four blocks of trials, each block consisting of 48 trials, 24 'Yes' or 'No' stimuli with a total duration of 6–7 min. The 'Yes' and 'No' stimuli were provided pseudo-randomly. The calibration for the motor imagery session consisted of two to four blocks of trials, each block consisting of 96 trials, with 'PHY' and 'MI' appearing pseudo-randomly for alternating physical movement and motor imagery, and 48 'Yes' and 48 'No' stimuli with a total duration of 12–13 min.

*2.2.2. Discrete two-dimensional-cursor-control game.* Sustained physical movement is usually associated with a persistent event-related desynchronization (ERD), while cessation of movement is followed by a beta band rebound above baseline power levels, i.e. event-related synchronization (ERS). Since we intended to discriminate ERD from ERS, which occurs only after cessation of movement in the T2 window, we only extracted EEG signal in the T2 time window to classify 'Yes' or 'No' intention determined from ERD and ERS. Successfully classifying the four kinds of movements in motor execution or motor imagery was the basis of the realization of 2D control.

In a 2D plane, the cursor can be moved in four directions: up, down, right and left, each of which was linked to one of the four movements. We intended to decode movement intentions to determine the subject's control of the cursor direction. As human movement intention is associated with spatial ERD and ERS (on either left or right hemisphere), we applied the detection strategy as shown in figure 2. For example, if the subject wanted to move the cursor to right, he needed to perform the 'RYes' task, either physical or motor imagery to develop an ERD pattern on the left hemisphere. When the associated ERD on the left hemisphere was detected in the T2 time window, the cursor would move in the right direction; similarly, if the subject wanted to move the cursor upward, he needed to perform the 'LNo' task, and when the associated ERS on the right hemisphere was detected in the T2 window, the cursor would move upward accordingly.

Upon successfully decoding movement intentions in the offline analysis, the subjects played a game of two-dimensional control of cursor movement on a computer monitor. A brief description of the 2D cursor-control game is given here since the detailed design of the online game was similar to the one given for binary cursor-control game (Bai *et al* 2008). The subjects were instructed to move the cursor to the target and avoid a designated 'trap'. The cues were presented in the same duration as that in the calibration session. Classification of 'Yes' and 'No' trials of right and left hands was used to direct 2D control correlated with cursor movement. As illustrated in figure 2, the detection of 'LYes' will direct the cursor move

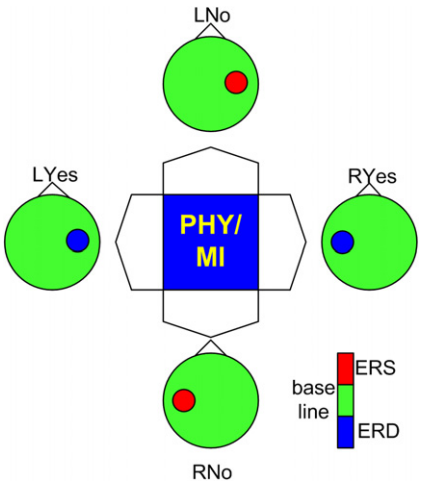


**Figure 2.** Scheme of 2D cursor control. Four directions control by spatial detection of ERD/ERS on the right/left hemisphere associated with intention to move or cease to move left/right hand. In order to control the cursor moving to left ('LYes' direction), the subjects may perform sustained physical movement/motor imagery so that ERD on the right hemisphere can be detected. Other direction controls are similar.

to the left, and similar with the other directions. The initial positions of cursor, target and trap were provided pseudo-randomly and the number of detections was different in each game. The subjects played 4–6 games and they were allowed 5–10 min to practice the game before the test.

In the online 2D game, the subjects determined the path to reach the target using their own game strategy. From the example shown in figure 3(a), the subject may choose to move to the right instead of downward in that situation. It was also possible that the subject would choose to move up to the margin of the grid and then move along the margin to the target. Due to various strategies, it was difficult to determine the cursor-control accuracy from the path of the cursor movement. Instead, in the case of physical movement, we used the EMG activity in the detection window to interpret whether the subjects desired to move to one of the four directions, and as a result, the control accuracy could quantitatively be determined from the actual cursor movement from the EEG derived results. In the case of motor imagery for online game, the subjects determined the direction to move; as there was no EMG activity of motor imagery, we were unable to know whether each movement was correctly decoded as the subject intended. Therefore, instead of quantitative measurement of control accuracy, we qualitatively evaluated the success of the two-dimensional cursor control with motor imagery by whether the subjects could control the cursor to reach the target. However, if the cursor was moved into the trap or the total number of moves reached the limit of five times the shortest possible moves, the game would automatically stop. We considered the successful judgment of the two-dimensional cursor control with motor imagery to be a qualitative measurement. The quantitative measurements of control accuracy for motor imagery were determined from the visually cued motor imagery of wrist extension, i.e. in the calibration procedure.

The main purpose for the proposed computer game was to improve the subjects' motivation in participating in the investigation. The subjects played the game with physical movements first. When the subjects were comfortable with the game, whether the subjects could play the game with motor imagery was determined.

*2.2.3. Mental strategy for motor imagery.* In the motor imagery part, the subjects were asked to imagine repetitive wrist extension of their own hands. As motor imagery is not a routine natural behavior in daily life, usually mental training with feedback is required before the subjects can perform a vivid imagination of the movement (Neuper *et al* 2009). In this study, there was no feedback in the calibration procedure for motor imagery and the modeling under the calibration data may be unreliable if the subjects were unable to imagine the physical movements. In order to achieve better calibration as well as modeling, the subjects performed both physical movement and motor imagery in the calibration step in the motor imagery session. Our assumption was that the subjects would be able to imagine more vividly right after a physical movement. However, only the data associated with motor imagery were used for offline calibration and modeling for the subsequent motor imagery study. In the motor imagery task, the subjects reported difficulty in imagining the termination of movement. We guided them to stop imagining movement by switching from the imagination of the motor task to a non-motor task such as reciting the alphabet or counting numbers mentally.

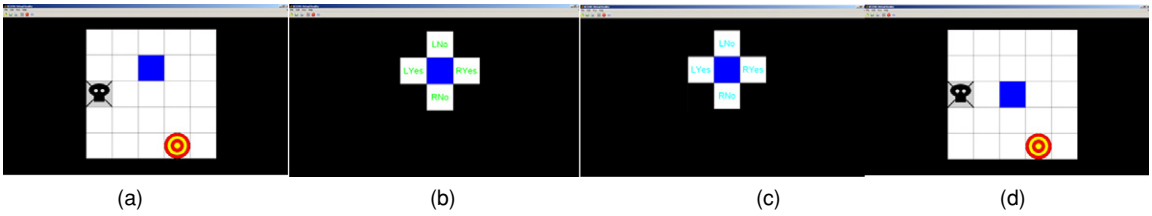


**Figure 3.** Paradigm of a discrete two-dimensional cursor-control game. (a) A game grid is displayed for 2–3 s showing a cursor (blue), target (red) and trap (black). (b) All squares except those adjacent to the cursor are masked and green prompts are displayed in the adjacent squares. (c) After a T1 delay, these prompts turn blue and remain for a period of T2. (d) The subject's response uniquely determines the cursor movement direction, which the cursor slides to. The entire process (a)–(d) then repeats for the next cursor move, and so on until the target is obtained, the trap is hit or too many moves have been made.

### *2.3. Data acquisition and online data processing system*

EEG was recorded from 27 (tin) surface electrodes (F3, F7, C3 A, C1, C3, C5, T3, C3P, P3, T5, F4, F8, C4 A, C2, C4, C6, T4, C4P, P4, T6, FPZ, FZ, FCZ, CZ, CZP, PZ and OZ) attached on an elastic cap (Electro-Cap International, Inc., Eaton, OH, USA) according to the international 10–20 system (Jasper and Andrews 1938), with reference from the right ear lobe and ground from the forehead. For surface electromyography (EMG), which was used to monitor the movement, two electrodes were filled with conductive gel and taped over the right and left wrist extensors. Electrodes for bipolar electrooculogram (EOG) above left eye and below right eye were also pasted.

Total duration of preparation included time to obtain informed consent, paradigm explanation, setting up the electrodes and preparations of hardware and software. This procedure took about 30 min to 1 h. Signals from all the channels were amplified (g.tec GmgH, Schiedlberg, Austria), filtered (0.1–100 Hz) and digitized (the sampling frequency was 250 Hz).

The digital signal was then sent to a HP PC workstation and was online processed using a home-made MATLAB (MathWorks, Natick, MA) Toolbox: brain–computer interface to virtual reality or BCI2VR (Bai *et al* 2008, 2007). The BCI2VR programs provided both the visual stimulus for the calibration and the two-dimensional cursor-control game, as well as the online processing of the EEG signal. The signal for decoding was extracted following the cues from the visual stimulus.

### *2.4. Computational methods for decoding movement intention*

Recent BCI studies reported that BCI performance in terms of both accuracy and efficiency can be further improved by applying advanced filters and more computationally intensive nonlinear classification methods (Muller-Gerking *et al* 1999, Naeem *et al* 2006). We have first employed simple linear methods, and then more intensive computational methods have been explored to determine whether and how the classification performance could be further improved.

The online signal processing to decode movement intention consists of three steps: (1) spatial filtering, (2) temporal filtering and (3) feature extraction and classification.

*Spatial filtering.* Surface Laplacian derivation (SLD) was applied. EEG signal from each electrode was referenced to the averaged potentials from the nearby four orthogonal electrodes (Hjorth 1975). SLD operation improves the localization of sources, by reducing the smearing effect in conducting layers of the head, and also reducing the common reference effect (Nunez *et al* 1997). Besides, the EEG feature of local synchrony, i.e., frequency power changes, can be enhanced as well (Pfurtscheller 1988). As a result, the spatial difference due to different hand movements might be more distinguishable.

*Temporal filtering.* The power spectral density was estimated from the spatially filtered EEG signal from the T2 window and according to the visual inspection of time–frequency plot of ERD and ERS (refer to Results session and figures 4 and 5), the time period 1 s–2 s after the T2 window started was extracted in order to obtain the strongest ERD/ERS. Because the signal was no longer stationary or associated with certain motor task outside a short-lasting data window, the data length for estimation was limited so that the natural power estimation of ERD and ERS under the periodogram method was not a consistent estimation with a variance as large as the true spectrum. The Welch method was applied with a Hamming window to reduce estimation variance and side-lobe effect (Welch 1967): the data in the selected time window were segmented and periodograms from all segments were averaged to obtain smoothed estimation. The length of the segment determining frequency resolution was compromised with the number of segments determining the estimation variance so that the segment length or the frequency bin width needed to be optimized. The optimization was performed using the cross-validation method with a MLD classifier. We found 4 Hz frequency resolution or a segment length of $256/4 = 64$ under 50% overlapping, provided a better classification of ERD and ERS across subjects, which was consistent with what we used for the binary control of 2D cursor movement (Bai *et al* 2007).

*Feature extraction and classification.* For either physical movement or motor imagery, there were about 96 trials making the data pool of 96 samples with 16 samples for each of the four classes. The offline performance of multi-class classification was evaluated from 10-fold cross-validation; 90% of the data pool was used for training, and the other 10% was used for validation so that the validation data set was independent of the training dataset. For classification methods using hyper-parameters or feature evaluation for feature selection, these parameters or features were also determined by the training data set only. In the online game, the features for decoding the movement intention were extracted and classified using the parameters determined from the calibration data set.

#### *2.4.1. Feature extraction*

*Empirical feature reduction.* Assuming that movement intention associated cortical activities occur over the motor cortex, we reduced the channel number from 29 to 14, which covered both left and right motor areas. Furthermore, as we did not expect relevant activities in the delta, theta and gamma bands, only alpha and beta band (8–30 Hz) activities were extracted for modeling and classification. Thus, the total number of extracted features was 8 (frequency bins) $\times$ 14 (channels) $= 112$ features.

*Bhattacharyya distance.* Bhattacharyya distance provides an index of feature separability for binary classification, which is proportional to the inter-class mean difference divided by intra-class variance (Chatterjee *et al* 2007). The empirically extracted features were ranked by the Bhattacharyya distance for further classification.

*Genetic algorithm.* Genetic algorithm (GA)-based feature selection is a stochastic search in the feature space guided

by the concept of inheriting, where at each search step, good properties of the parent subsets found in the previous steps are inherited. 10-fold cross-validation was used with a Mahalanobis linear distance (MLD) classifier for feature evaluation (Li and Doi 2006). In this approach, the population size we used was 20, the number of generations was 100, the crossover probability was 0.8, the mutation probability was 0.01 and the stall generation was 20.

#### 2.4.2. *Classification methods*

*Mahalanobis linear distance classifier*. Classification was done upon measuring the Mahalanobis linear distance, which computed a pooled covariance matrix averaged from individual covariance matrices in all task conditions where the discriminant boundaries were hyper-planes leaning along the regressions (Marques 2001). All 112 features after empirical feature reduction were used for calculating the distance in high-dimensional space.

*GA-based Mahalanobis linear distance classifier*. The sub-optimal feature subset was selected by GA, and the selected features providing the best cross-validation accuracy were applied to a Mahalanobis linear distance classifier. The number of features for the subset was 4, which was determined from the cross-validation accuracy with feature numbers of 2, 4, 6, 8 and 10 from the calibration data set of S1.

*Decision tree classifier*. Since a certain feature subset, for example, channels over the left motor cortex, may be sensitive to discriminate the intention to move the right hand and not sensitive for detecting other movement intentions, a decision tree method (DTC) was employed for the multi-class classification task in this study. At each level of DTC, the features for one-to-others classification were ranked by the Bhattacharyya distance, and the four features with higher ranks were used for classification by MLD. The number of features for classification was determined from preliminary comparison with numbers of 2, 4, 6, 8 and 10.

*Support vector machine classifier*. Support vector machine (SVM) tackles the principle of structure risk minimization with the consideration of maximization of the margin of separation (Vapnik 1998). As a consequence, SVM can provide a good generalization performance independent of the sample distribution. As a promising method, SVM has been suggested in a number of BCI applications (Olson *et al* 2005, Thulasidas *et al* 2006). We employed a SVM approach provided in LIBSVM (Fan *et al* 2005). The radial basis function was used as the SVM kernel function as it can provide a similar classification outcome compared with other kernels (Keerthi and Lin 2003). As the performance of SVM depends on the regulation parameters or hyper-parameters C and the width of the kernel $\sigma$ (Muller *et al* 2001, Chang and Lin 2001), 10-fold cross-validation was performed; $2^K$, $K$ from –5 to 15 with a step of 2 for the penalty parameter and $2^K$, $K$ from $-15$ to 5 with a step of 2 for the spread parameter. These parameters were determined by the training data set only.

### 2.5. *Data processing for neurophysiological analysis*

Offline data analysis was performed to investigate the neurophysiology following the tasks of 'Yes' and 'No' using the right or left hands. The calibration datasets were used for analysis. Data processing was performed using the MATLAB Toolbox of BCI2VR. Epoching was done with windows of $-2$ s–7 s with respect to the first cue onset. Any epochs contaminated with artifacts were rejected. ERD and ERS were calculated for each case. Epochs were linearly de-trended and divided into 0.256 s segments. The power spectrum of each segment was calculated using FFT with Hamming window resulting in a bandwidth of about 4 Hz. ERD and ERS were obtained by averaging the log power spectrum across epochs and baseline corrected with respect to $-2$ s–0 s.

## 3. Results

### 3.1. *Neurophysiological analysis of ERD/ERS*

The proposed BCI in this study intended to differentiate ERD and ERS patterns in two hemispheres following right-hand and left-hand movement or motor imagery. In the calibration session, for either hand, subjects performed motor execution or motor imagery during both T1 and T2 windows for the 'Yes' case, whereas they performed the same tasks during the T1 window and stopped to relax during T2 window for the 'No' case. The motor task was the same in the T1 window for both 'Yes' case and 'No' cases. The spatiotemporal analysis following the 'No' cue onset was performed for either hand using the calibration dataset for both motor execution and motor imagery.

Figure 4 shows examples of time–frequency plots, head topographies of ERDs or ERSs for motor execution with physical movement, from subjects 1, 2, 3 and 4, respectively. For each subject, time–frequency plots of channel C3 over the left sensorimotor cortex and C4 over the right hemisphere are illustrated in the left two columns and head topography of ERD or ERS to their right, containing each of the four situations: 'RYes', 'RNo', 'LYes' and 'LNo'. In the time–frequency plot, 0 s stands for the first cue (green in the visual paradigm) occurrence. ERD (blue color) was observed from around 0.5–1 s after the cue onset due to the response delay; for S1, S2 and S3, ERD in both alpha and beta bands from 10–30 Hz was observed over motor areas contralateral to the hand moved. The ERS in red color was mainly observed in the beta band centered around 20 Hz over the contralateral motor areas. Compared with ERD patterns, ERS was short-lasting in time but highly distinguishable. The ERD and ERS topography shows beta band activity: 21–24 Hz for S1 and S2 and 17–20 Hz for S3. Therefore, the ERD and ERS on either left or right hemisphere provided four spatial patterns to detect 'RYes', 'RNo', 'LYes' and 'LNo' intentions. However, ERD and ERS were less distinguishable for S4 (21–24 Hz for topography).

Figure 5 shows the time–frequency plots and head topography of ERD and ERS associated with motor imagery. Similar to the patterns associated with physical movement, ERD associated with motor imagery was observed in both

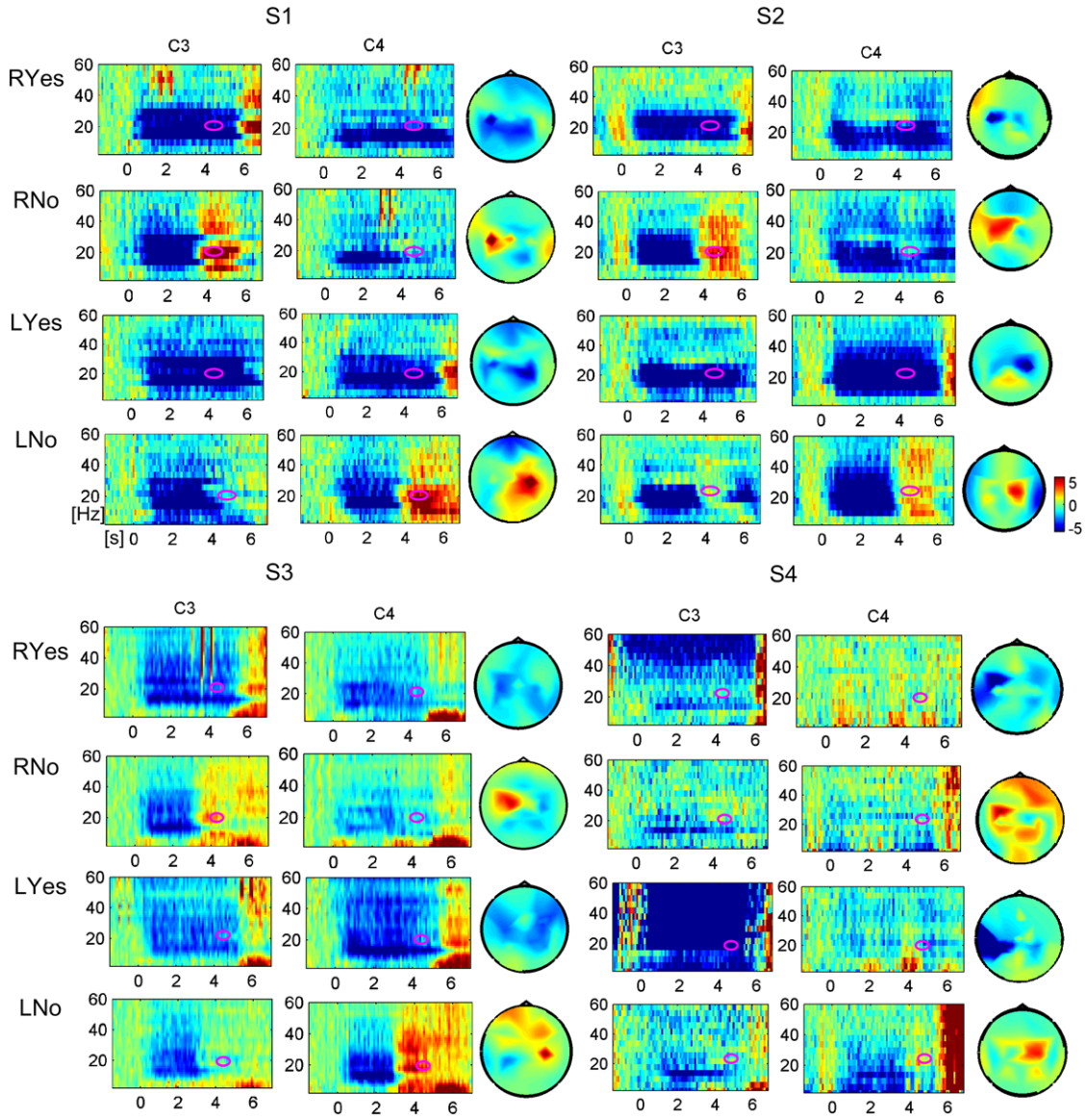


**Figure 4.** Time-course and topography of ERD and ERS during motor execution following the calibration paradigm for S1, S2, S3 and S4. Blue color stands for power decrease or ERD; red stands for power increase or ERS. The T1 window is from 0 s to 2.5 s and the T2 window is from 2.5 s to 5 s. For S1, S2 and S3, ERD was observed in the T2 window on the left hemisphere during sustained right-hand movement; ERS was observed in the T2 window on the left hemisphere when the subjects ceased to move right-hand movement. During left-hand movement, ERD was observed in the T2 window on the right hemisphere during sustained movement and ERS on the right hemisphere when the subjects ceased to move left hand. ERD and ERS in each case were marked by pink circles in the time–course plot. The head topography corresponding to the pink marked time period was provided next to the time–course plots.

alpha and beta bands on the contralateral hemisphere with the hand moved, although ERD amplitude was smaller than that of physical movement. ERS in the T2 window was observed on the contralateral hemisphere in beta band (13–24 Hz) only, and its amplitude was smaller than that of physical movement. During left hand motor imagery for S1 ('LYes'), ERD in the T2 time window was also observed on the left hemisphere. The ERD and ERS associated with motor imagery also provided four spatially differentiable patterns; however, the smaller amplitudes of ERD and ERS with motor imagery may result in less effective detection in single trials.

### *3.2. Feature analysis*

The best frequency bands and channels for classifying movement intentions were determined from the calibration data sets. Figure 6 shows the spatial-frequency feature analysis indexed by the Bhattacharyya distance for S1, S2, S3 and S4 during motor execution with physical movement, where all the channels over the whole head were used. The first column for each subject illustrates the channel–frequency plot of the Bhattacharyya distance, and the second column is the topography of the Bhattacharyya distance of the best

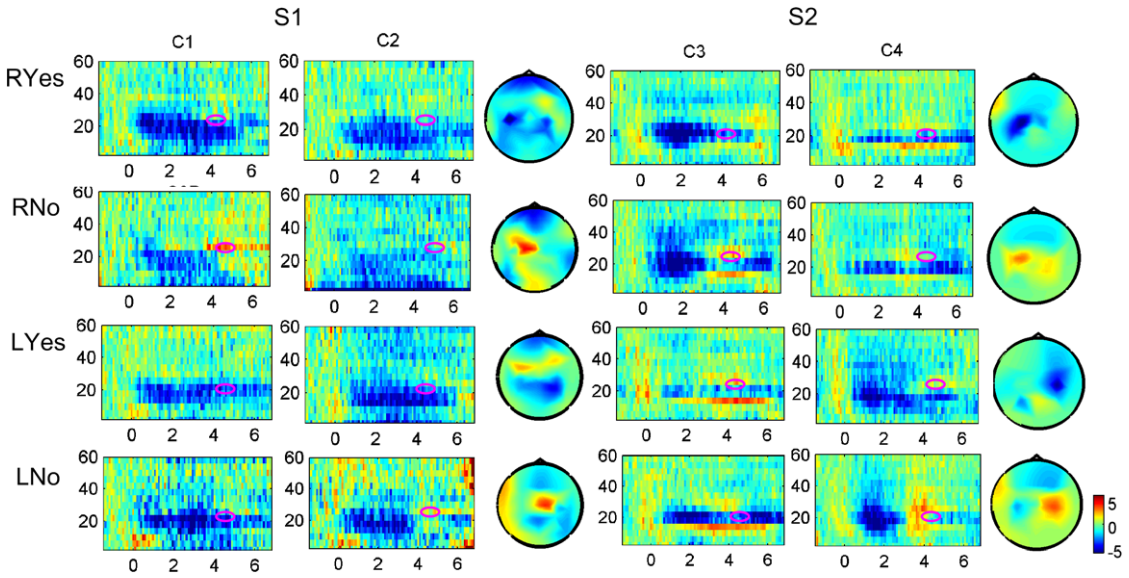


**Figure 5.** Time-course and topography of ERD and ERS during motor imagery following the calibration paradigm for S1 and S2. For both S1 and S2, ERD is obtained in the time window with sustained motor imagery and ERS with termination of motor imagery. ERDs appear in both alpha and beta bands, bilateral, whereas ERSs appear only in the alpha band on the contralateral hemisphere. ERD and ERS in each case were marked by pink circles in the time–course plot. The head topography corresponding to the pink marked time period is provided next to the time-course plots.

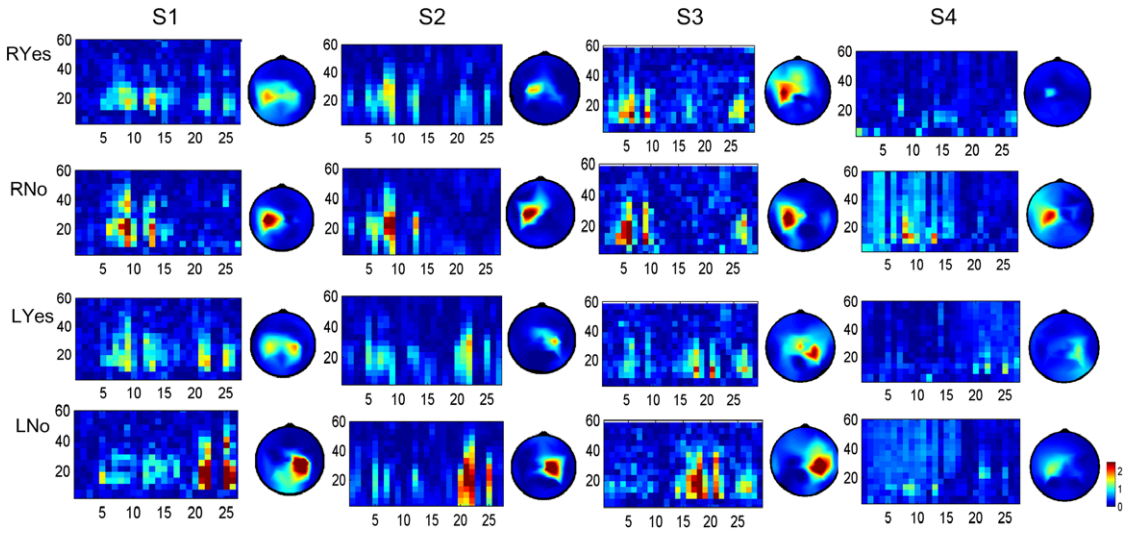


**Figure 6.** Feature visualization indexed by the Bhattacharyya distance for S1, S2, S3 and S4 during motor execution following the calibration paradigm. The best frequency band with the highest separability was found in the beta band, and the best channel was found in sensorimotor areas.

frequency band. In the Bhattacharyya distance plot, the dark red color shows the higher Bhattacharyya distance standing higher separability to classify movement intentions from single trial EEG signal.

In the channel–frequency plot for S1, the higher Bhattacharyya distance value for right-hand physical movement was observed in beta band ranging from 17 to 24 Hz in the channels located on the left hemisphere over the sensorimotor area. The high separability between ERD and ERS in the beta band was consistent with the time–frequency analysis in figure 4. The topography of the Bhattacharyya distance around 17–24 Hz shows that the best EEG spatial channels for the classification of 'RYes' and 'RNo' were in the contralateral left hemisphere over the sensorimotor area since ERS presented on contralateral left hemisphere only, although ERD occurred bilaterally as shown in figure 4. A higher Bhattacharyya distance value for left-hand physical movement was also seen in the beta band on the contralateral right hemisphere. For S2, the distribution of Bhattacharyya distance values was similar to that of S1, except that for either right hand or left hand, the 'Yes' case showed high separability only on the contralateral hemisphere, which can be seen in the topography of the Bhattacharyya distance. For S3, the best frequency band with the highest Bhattacharyya distance value was in the beta band around 13–24 Hz. The higher separability of the beta band activity was consistent with the ERD and ERS

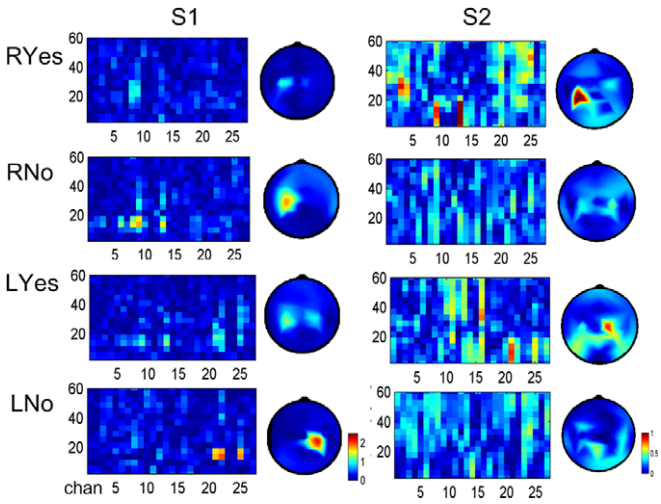


**Figure 7.** Feature visualization indexed by the Bhattacharyya distance for S1 and S2 during motor imagery following the calibration paradigm. The best frequency band with the highest separability was found in the beta band, and the best channel was found in sensorimotor areas.

features shown in figure 4, where both ERD and ERS were seen only in the beta band. For S4 with physical movement, the values of the Bhattacharyya distance were much smaller than other subjects, although the spatial pattern was similar. The lower Bhattacharyya distance indicates that the classification would be very difficult from single-trial signals.

Figure 7 shows feature analysis for S1 and S2 with motor imagery. For S1 and S2, the distribution of higher Bhattacharyya distance values was similar to that with physical movement, but the separability was lower. The highest Bhattacharyya distance values were in the beta band and on the channels over contralateral hemisphere for both right- and left-hand motor imagery.

### *3.3. Classification*

The comparison of 10-fold cross-validation accuracies using MLD, GA-MLD, DTC and SVM methods for S1, S2, S3 and S5 during physical movement is shown in table 1. Since ERD and ERS patterns were not strong enough for S4, we excluded it from further exploration of classification methods. MLD has a mean value of 70.2%; after applying genetic algorithm in feature selection, GA-MLD provides an improved mean value of 88.3%. Using a paired $t$-test, GA-MLD is found to have a significant improvement of the classification accuracy over the MLD ($t = 7.64$, df $= 3$, $p$-value $< 0.01^*$). Similarly, we also compared DTC and SVM performance with that of MLD. Paired $t$-test gives the result showing that DTC outperforms MLD significantly ($t = 4.20$, df $= 3$, $p$-value $< 0.03^*$) and SVM improved significantly better than MLD as well ($t = 5.56$, df $= 3$, $p$-value $< 0.02^*$).

Although the intensive methods GA-MLD (mean 88.3%), DTC (mean 86.4%) and SVM (mean 88.1%) all performed significantly, better than MLD (mean 70.2%), there was no significant difference among these three methods through one-way analysis of variance (ANOVA), $F(1,2) = 5.7$, $p$-value $< 0.39$, alpha $= 0.05$.

Since there was no significant difference among the intensive methods, the DTC method was employed for the online 2D cursor control game. Except for S4, all the other four subjects were successful in controlling the cursor moving to the target by physical movement and the average online game performances for S1, S2, S3 and S5 were 92%, 85%, 81% and 84%, with the overall performance of 85.5% $\pm$ 4.65%.

S1 and S2 participated in the second session performing motor imagery tasks. The offline classification accuracy for S1 was 73% $\pm$ 5.97%, and for S2 was 59.2% $\pm$ 3.63%, which were lower than those of cursor control with physical movement. The two subjects reported good concentration throughout the recording, except that S2 felt sleepy in a short period in the middle. Online 2D cursor control game using motor imagery was performed by S1 and S2. S1 was able to move the cursor to the target. However, S2 performed less well than S1. The performance was consistent with the classification results for motor imagery.

## 4. Discussion

### *4.1. Spatial detection of ERD and ERS*

We observed contralateral ERD and ERS in the beta band during sustained movements and post-movement from all subjects when they performed physical movements; ERD over the motor area on left hemisphere associated with sustained right-hand extension; post-movement ERS or beta band rebound occurring when stopping movement; ERD on right hemisphere associated with sustained left-hand extension and ERS with cessation of the movement. ERD and ERS patterns on left and right hemispheres were highly differentiable for subjects S1, S2, S3 and S5, whereas they were less detectable for S4. For motor imagery, S1 and S2 showed similar ERD/ERS patterns as those with physical movement. The amplitudes of ERD/ERS, however, were smaller. Although the ERD/ERS patterns were expected to be similar between physical movement and motor imagery, we considered that the effectiveness of motor imagery, i.e. how to vividly imagine limb movement, might highly affect cortical ERD/ERS patterns.

The reason for the fact that motor imagery has less robust performance than physical movement might be that motor imagery is not a natural behavior and thus requires more effort than performing physical movement. Besides, compared with physical movement, there is no neural feedback in motor imagery which may exhibit less activity (ERS) in the motor cortex and result in a lower signal to noise ratio. Considering that motor imagery is more meaningful for BCI application, training may be needed to enhance the involvement of subjects with motor imagery.

### *4.2. Decoding rate and accuracy*

The BCI performance can be evaluated from both the decoding rate and accuracy (Wolpaw *et al* 2002). Wolpaw *et al* introduced the information transfer rate (ITR) for a BCI as bits per minute (bpm) as a good measurement for both decoding rate and accuracy (Wolpaw *et al* 2000). In our study of 2D

**Table 1.** 10-fold cross-validation accuracy.

| Subject | MLD (%) | GA-MLD (%) | DTC (%) | SVM (%) |
|---|---|---|---|---|
| S1 | 63.1 ± 4.51 | 87.7 ± 1.29 | 87.8 ± 1.47 | 87.8 ± 1.31 |
| S2 | 79.5 ± 6.21 | 93.0 ± 1.97 | 85.5 ± 3.87 | 90.0 ± 3.12 |
| S3 | 67.3 ± 3.04 | 85.2 ± 0.95 | 84.5 ± 2.30 | 88.9 ± 1.04 |
| S5 | 71.0 ± 2.18 | 87.2 ± 0.58 | 87.7 ± 1.75 | 85.8 ± 2.13 |
| Average | 70.2 ± 6.97 | 88.3 ± 3.33 | 86.4 ± 1.64 | 88.1 ± 1.79 |

MLD, Mahalanobis linear discrimination; GA-MLD, genetic algorithm-based Mahalanobis linear discrimination; DTC, decision tree classifier; SVM, support vector machine classifier.

control, accuracies for physical movement ranged from 85.2% to 93.0% (given by GA-MLD, although not significantly better than DTC and SVM), with the average of 88.3%; for a four-class mental task, ITR was from 1.16 bits per trial, to 1.37 bits per trial, with the average 1.29 bits per trial. For motor execution with physical movement, the total duration of T1 and T2 windows was 5 s, i.e. 12 trials per minute. Therefore, the ITR was 13.9–16.5; the average was 15.5 bits per minute. Similarly, for motor imagery, the ITR was 4.15 bits per minute to 8.03 bits per minute. The cueing period T1 is important as it left enough time for the subjects to prepare for the movement. The results were comparable in terms of both accuracy and decoding rate with previous studies (see review in Wolpaw *et al* (2002)). We consider that the T1 window can be further shortened or optimized when the subjects can make rapid response, and as a result, the ITR can be further improved. We also consider that the control performance/accuracy is very important in practical BCI application. As BCI is intended for patients having limited motor function which features extremely slowness in motor control, it may be appropriate to have limited communication speed, whereas the accuracy needs to be high enough so that the users may avoid frustration when using BCI.

Invasive methods using spike train or local field potentials (Donoghue 2002, Carmena *et al* 2003), or at least semi-invasive method using ECoG (Schalk *et al* 2008), have been investigated as the major signal methods for two-dimensional (or three-dimensional) BCI control. The noninvasive signal method, though more convenient for practical application, has been less studied. This study provides further evidence for two-dimensional BCI control using the noninvasive method. From spatial detection of ERD and ERS, two-dimensional control was reliable with a detection accuracy of 80–90%.

Previous 2D control was achieved by accurate control of EEG frequency power so that long-term training was required before the subject was able to regulate EEG rhythm precisely. In the proposed BCI methods, BCI cursor control was achieved by the ERD and ERS associated with natural motor behavior so that long-term training was no longer required.

### *4.3. Difficulty and improvement*

Unlike in binary motor imagery (Bai *et al* 2008) where the subjects imagine the movement of only one limb of the body, motor imagery in 2D motor control tasks can be more difficult, since the subjects need to respond quickly to each imagery task and switch reactions successfully among the four tasks. Fatigue is a common issue during data collection which requires a relatively long time and repetitive motor tasks. To maximize subject involvement so that they are highly motivated, the paradigm can be further improved in terms of a better design and a shorter calibration time, which will greatly benefit BCI application. Also, the subjects can be trained more as to how to avoid fatigue in the experiments. These issues will be considered and addressed in the subsequent studies.

### *4.4. Possible contamination of muscle artifact*

EMG contamination from facial muscles may possibly cause serious problems in BCI development (McFarland *et al* 2005). Throughout the experiment, EMG signal was monitored for all subjects, to make sure correct movements were performed and no EMG occurred during motor imagery. Further, the signal for classification was extracted from around 3.5 s–4.5 s with respect to the first color cue onset (i.e., 1 s–2 s after T2 started) so that the artifact contaminated signal outside this period was not included; feature analysis showed that beta activities restricted to motor areas were used for classification. Therefore, the EMG contamination was not a concern in this study.

### *4.5. Classification method analysis*

Mahalanobis linear distance uses a large number of features for classification. In multi-class classification tasks, a very large data set is used for proper training, and further, a feature subset may perform well for some classes but poorly for others. 'DTC' has been employed for overcoming these difficulties, to use multi-level classification under the 'divide and conquer' principle. Support vector machine (SVM) approach also provides good control of model complexity to avoid over-fitting, but due to the requirement for determining hyper-parameters, the training time in offline modeling might be longer. Furthermore, determining hyper-parameters may need a larger sample set. Taking into account all these considerations, 'DTC' would be preferable for online 2D cursor control, since it has good performance and is simple and fast.

### *4.6. Implications of proposed BCI*

BCI has been proposed for patients who may lose voluntary muscle contraction. In the extreme state such as in patients

with amyotrophic lateral sclerosis (ALS), individuals may be entirely 'locked-in' though their cognition is still intact. Under these conditions, BCI is then only possible with motor imagery. The two-dimensional BCI control in this study shows that reliability or accuracy was less with motor imagery than with physical movement. However, only two subjects have been studied with motor imagery so that further study with more subjects should be addressed. For patients who are not in a 'locked-in' state but cannot produce reliable muscle contraction due to muscle weakness or spasticity, we would expect more reliable two-dimensional control with their limited motor output as this study demonstrates a highly reliable control with simple physical movement.

In this study, the set-up time for electrodes over the whole scalp was around 15–20 min. As this is an exploration study, we applied electrodes over the whole scalp. From the feature analysis in figure 6, we found the electrodes over the motor cortex provided better features for classification. Therefore, the number of electrodes for future practical application can be further reduced and the electrode setup time might be reduced to within 10 min.

In summary, ERD/ERS using our 2D natural paradigm present four distinguishable patterns as we expected, both in physical movement and imagery. Although variability might lead to considerable challenges in the classification process, the intensive methods we applied exhibit satisfying properties and robust results, making 2D control more reliable. It is worthwhile pursuing this potential system since EEG is less expensive, flexible, and has established analysis techniques. If the design and signal processing methods can be further improved, BCI products will eventually offer those who have totally lost muscle control convenient, fast and reliable control of mechanical devices. This will largely reduce the reliance on continuous support from others, and thus enhance their quality of life.

## References


Bai O, Lin P, Vorbach S, Floeter M K, Hattori N and Hallett M 2008 A high performance sensorimotor beta rhythm-based brain–computer interface associated with human natural motor behavior *J. Neural Eng.* **5** 24–35

Bai O, Lin P, Vorbach S, Li J, Furlani S and Hallett M 2007 Exploration of computational methods for classification of movement intention during human voluntary movement from single trial EEG *Clin. Neurophysiol.* **118** 2637–55

Bai O, Mari Z, Vorbach S and Hallett M 2005 Asymmetric spatiotemporal patterns of event-related desynchronization preceding voluntary sequential finger movements: a high-resolution EEG study *Clin. Neurophysiol.* **116** 1213–21

Birbaumer N, Murguialday A R and Cohen L 2008 Brain–computer interface in paralysis *Curr. Opin. Neurol.* **21** 634–8

Carmena J M, Lebedev M A, Crist R E, O'Doherty J E, Santucci D M, Dimitrov D, Patil P G, Henriquez C S and Nicolelis M A 2003 Learning to control a brain–machine interface for reaching and grasping by primates *PLoS Biol.* **1** E42

Chang C C and Lin C J 2001 Training nu-support vector classifiers: theory and algorithms *Neural Comput.* **13** 2119–47

Chatterjee A, Aggarwal V, Ramos A, Acharya S and Thakor N V 2007 A brain–computer interface with vibrotactile biofeedback for haptic information *J. Neuroeng. Rehabil.* **4** 40

Dobkin B H 2007 Brain–computer interface technology as a tool to augment plasticity and outcomes for neurological rehabilitation *J. Physiol.* **579** 637–42

Donoghue J P 2002 Connecting cortex to machines: recent advances in brain interfaces *Nat. Neurosci.* **5** (Suppl) 1085–8

Hjorth B 1975 An on-line transformation of EEG scalp potentials into orthogonal source derivations *Electroencephalogr. Clin. Neurophysiol.* **39** 526–30

Jasper H H and Andrews H L 1938 Electro-encephalography. III. Normal differentiation of occipital and precentral regions in man *Arch. Neurol. Psychiat.* **39** 95–115

Keerthi S S and Lin C 2003 Asymptotic behaviors of support vector machines with Gaussian kernel *Neural Comput.* **15** 1667–89

Krusienski D J, Schalk G, McFarland D J and Wolpaw J R 2007 A mu-rhythm matched filter for continuous control of a brain–computer interface *IEEE Trans. Biomed. Eng.* **54** 273–80

Lebedev M A and Nicolelis M A 2006 Brain–machine interfaces: past, present and future *Trends Neurosci.* **29** 536–46

Leeb R, Lee F, Keinrath C, Scherer R, Bischof H and Pfurtscheller G 2007 Brain–computer communication: motivation, aim, and impact of exploring a virtual apartment *IEEE Trans. Neural Syst. Rehabil. Eng.* **15** 473–82

Li Q and Doi K 2006 Analysis and minimization of overtraining effect in rule-based classifiers for computer-aided diagnosis *Med. Phys.* **33** 320–8

Marques J P 2001 *Pattern Recognition: Concepts, Methods and Applications* (Berlin: Springer)

McFarland D J, Sarnacki W A, Vaughan T M and Wolpaw J R 2005 Brain–computer interface (BCI) operation: signal and noise during early training sessions *Clin. Neurophysiol.* **116** 56–62

McFarland D J and Wolpaw J R 2003 EEG-based communication and control: speed–accuracy relationships *Appl. Psychophysiol. Biofeedback* **28** 217–31

Muller-Gerking J, Pfurtscheller G and Flyvbjerg H 1999 Designing optimal spatial filters for single-trial EEG classification in a movement task *Clin. Neurophysiol.* **110** 787–98

Muller K R, Mika S, Ratsch G, Tsuda K and Scholkopf B 2001 An introduction to kernel-based learning algorithms *IEEE Trans. Neural Netw.* **12** 181–201

Naeem M, Brunner C, Leeb R, Graimann B and Pfurtscheller G 2006 Separability of four-class motor imagery data using independent components analysis *J. Neural Eng.* **3** 208–16

Neuper C, Scherer R, Reiner M and Pfurtscheller G 2005 Imagery of motor actions: differential effects of kinesthetic and visual-motor mode of imagery in single-trial EEG *Brain Res. Cogn. Brain Res.* **25** 668–77

Neuper C, Scherer R, Wriessnegger S and Pfurtscheller G 2009 Motor imagery and action observation: modulation of sensorimotor brain rhythms during mental control of a brain–computer interface *Clin. Neurophysiol.* **120** 239–47

Nunez P L, Srinivasan R, Westdorp A F, Wijesinghe R S, Tucker D M, Silberstein R B and Cadusch P J 1997 EEG coherency: I. Statistics, reference electrode, volume conduction, Laplacians, cortical imaging, and interpretation at multiple scales *Electroencephalogr. Clin. Neurophysiol.* **103** 499–515

Oldfield R C 1971 The assessment and analysis of handedness: the Edinburgh inventory *Neuropsychologia* **9** 97–113

Olson B P, Si J, Hu J and He J 2005 Closed-loop cortical control of direction using support vector machines *IEEE Trans. Neural Syst. Rehabil. Eng.* **13** 72–80

Pfurtscheller G 1988 Mapping of event-related desynchronization and type of derivation *Electroencephalogr. Clin. Neurophysiol.* **70** 190–3

Pfurtscheller G and Solis-Escalante T 2009 Could the beta rebound in the EEG be suitable to realize a 'brain switch'? *Clin. Neurophysiol.* **120** 24–9

Rao S M *et al* 1993 Functional magnetic resonance imaging of complex human movements *Neurology* **43** 2311–8

Schalk G, Miller K J, Anderson N R, Wilson J A, Smyth M D, Ojemann J G, Moran D W, Wolpaw J R and Leuthardt E C 2008 Two-dimensional movement control using electrocorticographic signals in humans *J. Neural Eng.* **5** 75–84

Stancak A Jr and Pfurtscheller G 1996 Event-related desynchronisation of central beta-rhythms during brisk and slow self-paced finger movements of dominant and nondominant hand *Brain Res. Cogn. Brain Res.* **4** 171–83

Thulasidas M, Guan C and Wu J 2006 Robust classification of EEG signal for brain–computer interface *IEEE Trans. Neural Syst. Rehabil. Eng.* **14** 24–9

Vapnik V N 1998 *Statistical Learning Theory* (New York: Wiley)

Velliste M, Perel S, Spalding M C, Whitford A S and Schwartz A B 2008 Cortical control of a prosthetic arm for self-feeding *Nature* **453** 1098–101

Welch P D 1967 The use of fast Fourier transform for the estimation of power spectra: a method based on time averaging over short, modified periodograms *IEEE Trans. Audio Electroacoust.* **15** 70–3

Wolpaw J R, Birbaumer N, Heetderks W J, McFarland D J, Peckham P H, Schalk G, Donchin E, Quatrano L A, Robinson C J and Vaughan T M 2000 Brain–computer interface technology: a review of the first international meeting *IEEE Trans. Rehabil. Eng.* **8** 164–73

Wolpaw J R, Birbaumer N, McFarland D J, Pfurtscheller G and Vaughan T M 2002 Brain–computer interfaces for communication and control *Clin. Neurophysiol.* **113** 767–91

Wolpaw J R and McFarland D J 2004 Control of a two-dimensional movement signal by a noninvasive brain–computer interface in humans *Proc. Natl Acad. Sci. USA* **101** 17849–54